

Environmental hydrodynamic modeling applied to extreme events in Caribbean and Mediterranean countries

J. Lugon Jr.^{a,*}, M.M. Juliano^b, I. Kyriakides^c, E.N. Yamasaki^d, P.P.G.W. Rodrigues^e,
A.J. Silva Neto^f

^aEnvironmental Engineering Graduate Program, Instituto Federal Fluminense, Macaé, RJ, Brazil, email: jljunior@iff.edu.br (J. Lugon Jr.)

^bInstitute of Marine Research, University of Azores, Ponta Delgada, Azores, Portugal, email: manuela.juliano@gmail.com (M.M. Juliano)

^cDepartment of Engineering, University of Nicosia, Nicosia, Cyprus, email: kyriakides.i@unic.ac.cy (I. Kyriakides)

^dDepartment of Life and Health Sciences, University of Nicosia, Nicosia, Cyprus, email: yamasaki.e@unic.ac.cy (E.N. Yamasaki)

^eDepartment of Computational Modelling, Universidade do Estado do Rio de Janeiro, Nova Friburgo, RJ, Brazil,

email: pwatts@iprj.uerj.br (P.P.G.W. Rodrigues)

^fDepartment of Mechanical and Energy Engineering, Universidade do Estado do Rio de Janeiro, Nova Friburgo, RJ, Brazil,

email: ajsneto@iprj.uerj.br (A.J. Silva Neto)

Received 15 October 2019; Accepted 10 March 2020

ABSTRACT

There has been in recent years an increase in interest and concerns about natural disasters, both in the scientific community and the society, in relation to their frequency and intensity, the association to global warming, and cyclones (hurricanes and medicanes). In this work, two environmental hydrodynamics models are presented. The first model is built for Hurricane Irma that took place in 2017 in the Caribbean and the second for medicane Zorba that took place in 2018 in the Mediterranean Sea. The models were developed using downscaling techniques on the MOHID platform (a free open model developed for hydrodynamic solution). Water surface currents results are presented for regions of interest together with water level variations in Virtual Maregraphic Stations, “Isabella de Sagua” at Sagua de la Grande in Cuba, Key West in USA, Katacolon and “Kalamai” in Greece, all of them located in the trajectory of both cyclones. Promising results on the modeling of the interaction between water and the atmosphere aligned with available open-source data demonstrate the accuracy of inverse problem-based solutions for natural disaster modeling and its potential for drift simulation of floating objects in future studies.

Keywords Natural hazards; Hurricane; Cyclone; Medicane; Simulation; MOHID

1. Introduction

The Intergovernmental Panel on Climate Change IPCC claims the existence of scientific evidence about global warming and human-caused greenhouse gas emissions [1]. Additionally, a strong scientific interest in natural disasters, such as hurricanes and medicanes [2–4], is observed in the literature with the aim to understand their relationship with

global warming and the possible increment of their frequency and intensity [2–4]. Hurricanes are extreme natural events with potentially devastating effects on society, both in terms of property damage and loss of human life. In the Caribbean countries, hurricanes are particularly frequent phenomena, and, therefore, the great scientific effort is devoted to modeling and forecasting such events. According

* Corresponding author.

to the National Oceanic and Atmospheric Administration (NOAA-USA), Hurricanes Harvey, Irma, and María have inflicted severe damage with costs estimated at U\$265 billion [5]. On the other hand, medicanes are cyclones over the Mediterranean Sea, and are rare, smaller in size than tropical hurricanes, but with a similar structure. Even though at present such events are infrequent, they may become more frequent in the future as an effect of climate change [6]. Medicanes combine intense winds and heavy precipitation, and, therefore, can also produce significant damage [7]. In this work, the environmental hydrodynamics in the Caribbean and Mediterranean Seas are modeled using downscaling techniques on the MOHID platform [8,9]. The first critical extreme event of interest was Hurricane Irma (2017), with a significant impact on Caribbean countries, such as Barbuda, Puerto Rico, and Cuba, while the second one was the medicane Zorba, with significant impact on Greece (2018).

The objective of the present work is to compare water level measurements and model results for those two extreme events, using open free data and modeling tools, to be used in the near future in the formulation and solution of Inverse Problems for drift simulation of floating objects with relevant applications such as plastic, oil, or pollutants transport.

2. Methods

The MOHID (MOdelagem HIDrodinâmica – Hydrodynamic Modeling) Platform is a computational tool for hydrodynamic simulation, that is capable of simulating the transport of components in suspension and solution. The tool has been used to simulate complex features present in outflows observed in several coastal and estuarine areas [8–12]. MOHID’s source code can be downloaded from the website www.mohid.com.

In MOHID’s geometry module the vertical spatial discretization uses different coordinate systems which can be Sigma, Cartesian, or both combined. The sigma coordinate system applied alone at the first level, allows a more

convenient representation of the ocean/sea bottom near the coast. In the present work, a combination of these two coordinate systems (Sigma and Cartesian) is adopted for the second level, while sigma is adopted as the top domain and Cartesian is used to represent the bottom. Fig. 1 presents the Sigma and Cartesian coordinate systems used in the second level.

The three-dimensional hydrodynamic model available in the MOHID water solves the Navier–Stokes equations [Eqs. (1)–(4)] considering the Boussinesq and hydrostatic approaches [9].

$$\frac{\partial u_i}{\partial x_i} = 0 \tag{1}$$

$$\frac{\partial u_1}{\partial t} + \frac{\partial(u_j u_1)}{\partial x_j} = f u_1 - g \frac{\rho_\eta}{\rho_0} \frac{\partial \eta}{\partial x_1} - \frac{1}{\rho_0} \frac{\partial p_s}{\partial x_1} - \frac{g}{\rho_0} \int_s^\eta \frac{\partial \rho'}{\partial x_1} \partial x_3 + \frac{\partial}{\partial x_j} \left(v_h \frac{\partial u_1}{\partial x_j} \right) \tag{2}$$

$$\frac{\partial u_2}{\partial t} + \frac{\partial(u_j u_2)}{\partial x_j} = f u_2 - g \frac{\rho_\eta}{\rho_0} \frac{\partial \eta}{\partial x_2} - \frac{1}{\rho_0} \frac{\partial p_s}{\partial x_2} - \frac{g}{\rho_0} \int_s^\eta \frac{\partial \rho'}{\partial x_2} \partial x_3 + \frac{\partial}{\partial x_j} \left(v_h \frac{\partial u_2}{\partial x_j} \right) \tag{3}$$

$$\frac{\partial p}{\partial x_3} = -\rho g \tag{4}$$

where u_i are the velocity components in the Cartesian directions x_i , η is the elevation of free surface, f is the Coriolis parameter, v_h is the turbulent viscosity, p_s is the atmospheric pressure, and ρ is the reference density, ρ' is the specific mass anomaly, and ρ_η is the density at the free surface.

The equation obtained for free surface is derived by the integration of the equation of continuity in the water column:

$$\frac{\partial \eta}{\partial t} = -\frac{\partial}{\partial x_1} \int_{-h}^\eta u_1 dz - \frac{\partial}{\partial x_2} \int_{-h}^\eta u_2 dz \tag{5}$$

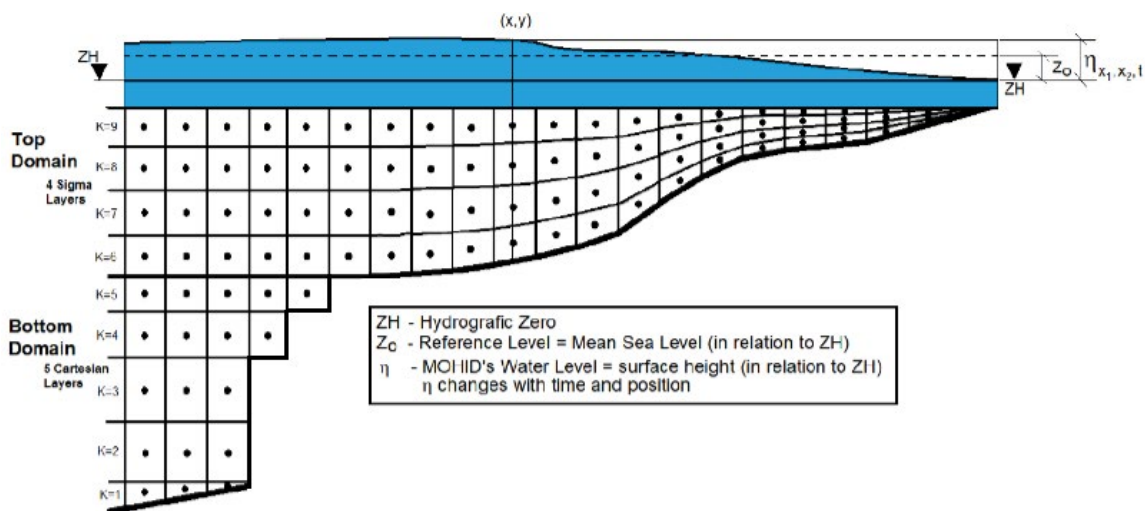


Fig. 1. Representation example of the spatial discretization and MOHID’s coordinate systems.

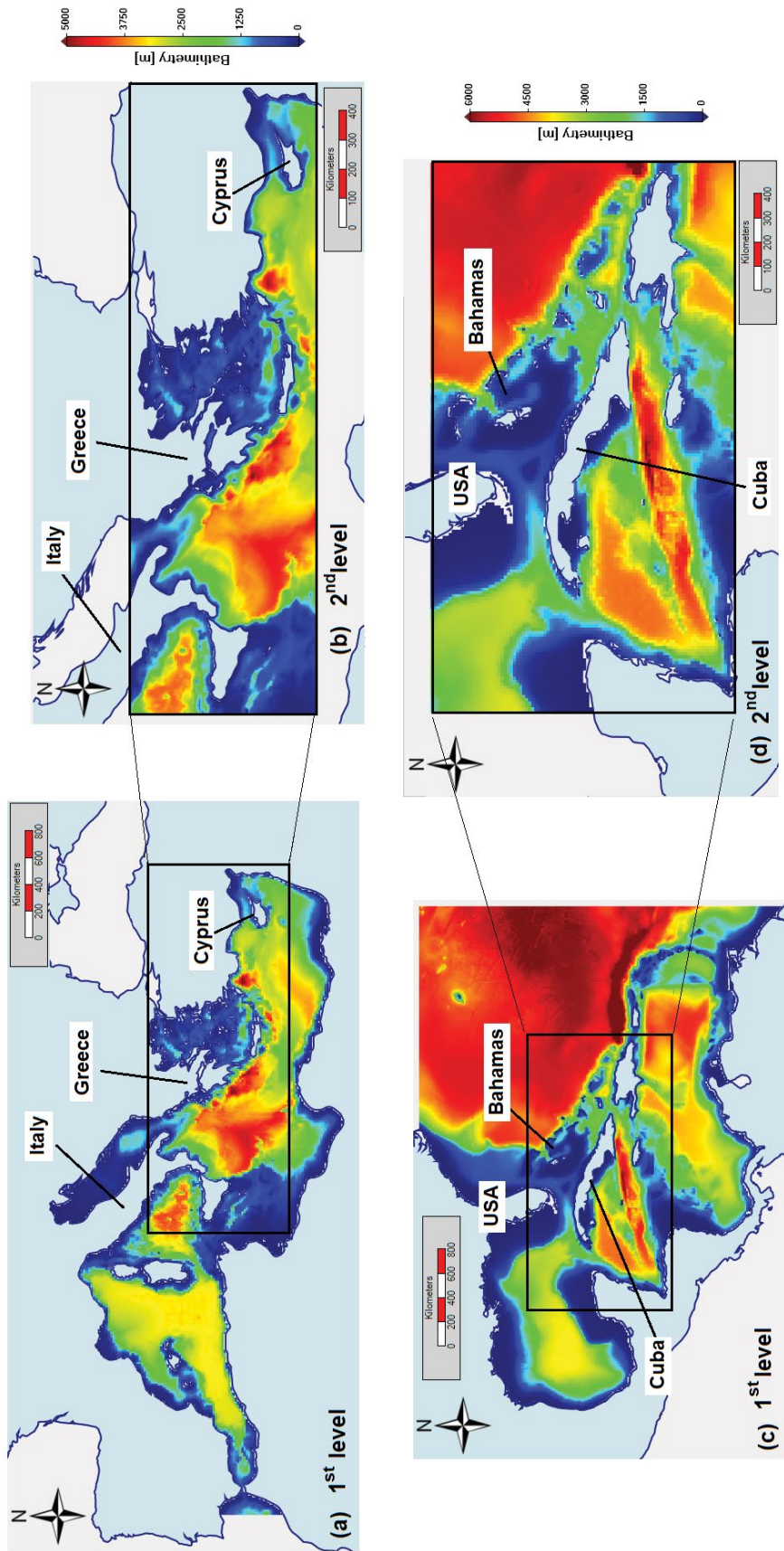


Fig. 2. Bathymetric maps of the first and second levels for Mediterranean (a and b) and Caribbean (c and d) regions.

where η is the free surface elevation and $-h$ is the bottom depth.

The model also solves the transport equation for any properties (θ), like salinity and temperature (Eq. (6)).

$$\frac{\partial \theta}{\partial t} + \frac{\partial (u_i \theta)}{\partial x_i} = \frac{\partial}{\partial x_i} \left(K \frac{\partial \theta}{\partial x_i} \right) + F_\theta \quad (6)$$

where K is the diffusivities of θ and F are the possible sinks or sources.

Fig. 2 presents the 1st and the 2nd levels of down-scaled bathymetric maps considered for the Northeastern Mediterranean region (a, b) and for the Western Caribbean Sea (c, d). Both models use a horizontal 0.12° grid discretization in the first level (a, c). For the second level, the Northeastern Mediterranean model uses a 0.04° grid discretization (b) and the Caribbean model keeps the 0.12° grid discretization, as used in the first level.

The Caribbean and Mediterranean Hydrodynamic Models described in this work used bathymetric information from GEMCO [13], atmospheric data from GFS [14], tidal components from FES2012 [15], and oceanographic data from the Copernicus Project [16]. The GOTM (General Ocean Turbulence Model), with the $k-\varepsilon$ model for the turbulent kinetic energy, is used to calculate the viscosity and diffusivity coefficients [17]. The downscaling technique was used for both models (Caribbean and Mediterranean) with two levels. In the first level, tidal data are forced (barotropic model) to compute values that are imposed on the subsequent level that constitute the downscaled baroclinic model. This approach is often applied to simulate oceanic hydrodynamics, where the flow is influenced by density variations. The Open Boundary Conditions (OBC) in both nested downscaling models are set according to each domain [9].

3. Results and discussion

3.1. Caribbean model

For the evaluation of the effects caused by the Hurricane Irma two Virtual Maregraphic Stations, “Isabela de Sagua” (Longitude = -80.02° ; Latitude = 22.93°) in Cuba and “Key West” (Longitude = -80.02° ; Latitude = 22.93°) in the USA were positioned in the model to capture the water level variation [18,19]. In Fig. 3, their locations are shown using the same bathymetric map already presented in Fig. 2d, zoomed in the area of interest.

Figs. 4a and b show the velocity modulus for the wind in the atmosphere (top figures) and the water surface currents (bottom figures), calculated with the Caribbean model for the time period from September 6th to 8th, 2017 and September 9th to 11th 2017, respectively.

It is important to note in Figs. 4a and b that the hurricane Irma appeared in the atmosphere at a large distance from the hydrodynamic domain in September 6th and 7th, and then it approached Cuba between September 9th and 10th. The effects of the high wind velocities are seen in the water surface currents, particularly on September 10th when it hit Cuba along the coastline. After that time period, hurricane Irma hit the USA on September 11th before vanishing.

Fig. 5 shows the water level variation at the “Key West” Maregraphic Station, located in Florida, USA, for a time period that includes the passage of Hurricane Irma for both MOHID modeled results and measurements from Sea Level Station Monitoring Facility [19]. It is possible to observe an unexpected rising of water level that coincides with the passage of the hurricane, even during a period of moderate astronomical tides (neap tides), between September 8th and 11th 2017.

In Fig. 6, the water level variation is shown at the Virtual Maregraphic Station “Isabela de Sagua” [18], located in Sagua la Grande, Cuba for a time period that includes the passage of Hurricane Irma, experimental measurements were not available for “Isabela de Sagua” Station. It is possible to observe an unexpected rising of water level that coincides with the passage of the hurricane, even during a period of moderate astronomical tides (neap tides), between September 8th and 11th 2017. The effects caused by the Hurricane Irma are more intense than what is observed for Key West Station, but experimental measurements are not available for comparison.

3.2. Mediterranean model

The evaluation of the effects caused by the medicane Zorba was performed using two Virtual Maregraphic Stations, “Kalamai” located in Kalamata (Longitude = 22.12° ; Latitude = 37.02°) and “Katacolo” (Longitude = 21.32° ; Latitude = 37.64°), both positioned in the model to capture the water level variation [20,21]. In Fig. 7, it is shown their locations in Greece using the same bathymetric map already presented in Fig. 2b, but now with a zoom in the area of interest.

Figs. 8a and b show the velocity moduli for the wind in the atmosphere (top figures) and the water surface currents calculated with the Mediterranean model (bottom figures) are represented for the time period between September 27th and 29th 2018, and September 30th to October 2nd, 2018, respectively.

It is important to note in Fig. 8a that the hurricane Zorba is formed in the atmosphere between September 27th and 28th and then it hit Greece on September 29th. Again, as it was observed in the Caribbean model, the effects of the high wind velocities are seen in the water surface currents.

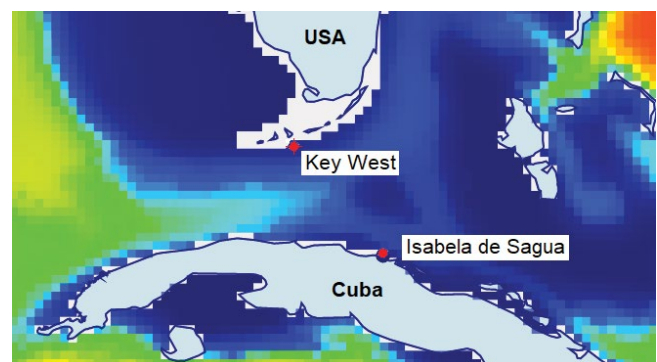


Fig. 3. Representation of the Virtual Maregraphic Stations “Isabela de Sagua” in Sagua la Grande (Cuba) and “Key West” in Florida (USA).

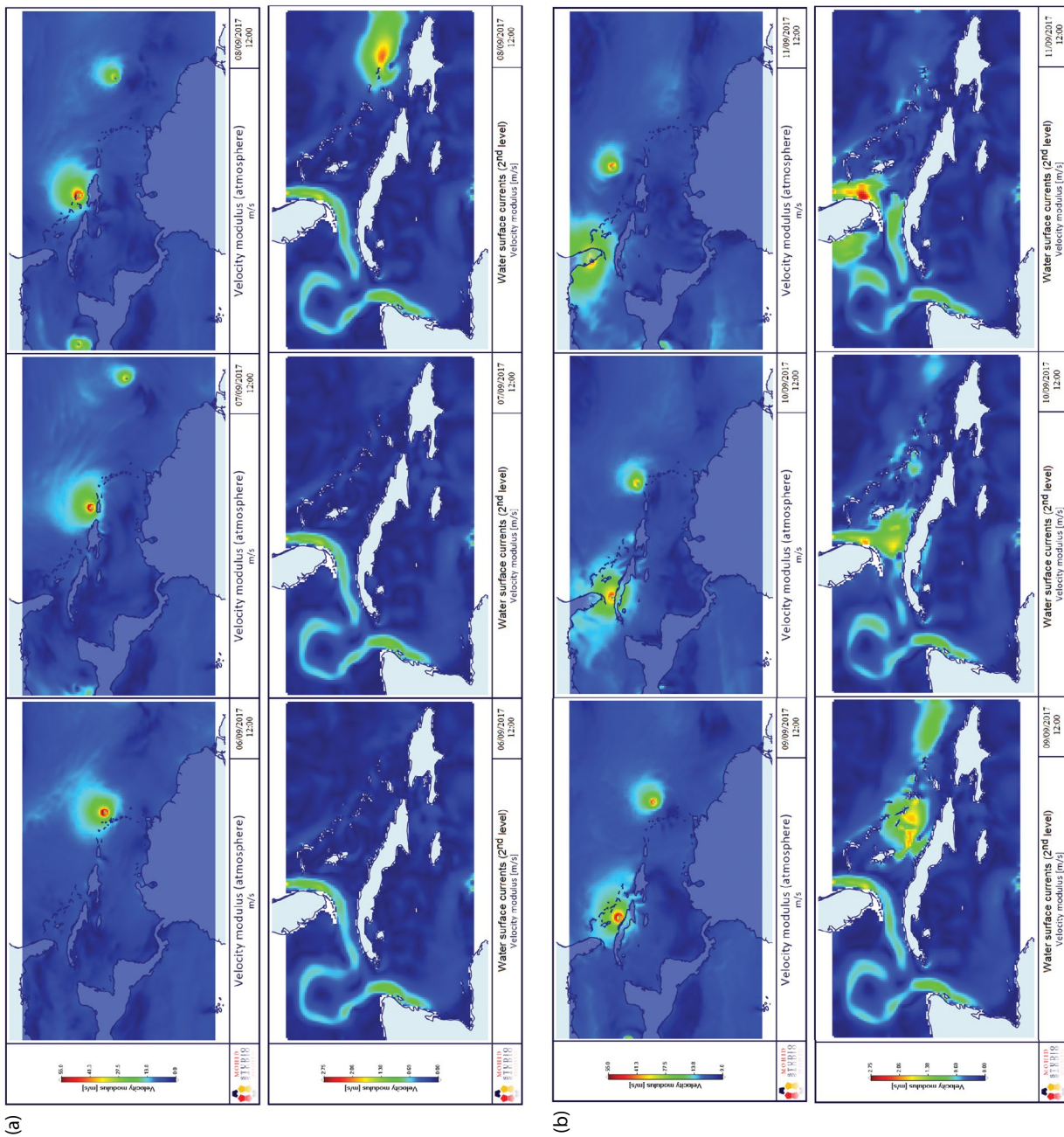


Fig. 4. Velocity moduli obtained from GFS [10] and results calculated for the water surface currents with MOHID [4,5] for the Caribbean model during the time period between (a) September 6th and 8th 2017 and (b) September 9th and 11th 2017.

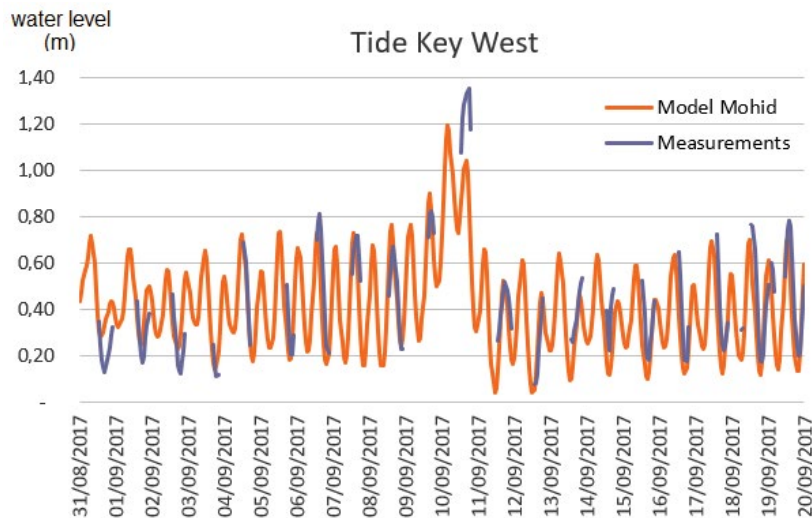


Fig. 5. Water Level (partial data available) measurements and model results for the Key West Station in Florida (USA). Hurricane Irma.

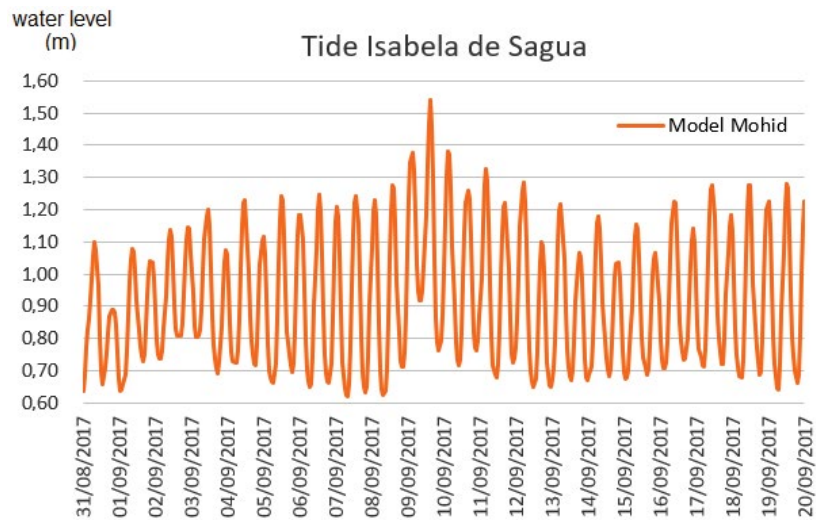


Fig. 6. Water Level Results Calculated for a Virtual Station located at Isabela de Sagua, Cuba. Hurricane Irma.

In Fig. 8b the hurricane Zorba is shown to pass throughout the Greek territory and dissipate between September 30th to October 2nd.

Fig. 9 shows the water level variation at the Maregraphic Station “Katacolo” in Greece, for a time period that includes the passage of the medicane Zorba nearby, both MOHID modeled results and measurements from Sea Level Station Monitoring Facility [21] are plotted. It is possible to observe that the model was able to capture the rising of water level that coincides with the passage of the medicane Zorba and that afterwards this effect vanishes and the water level comes back to usual astronomic tidal variation.

In Fig. 10, it is shown the water level variation at the Virtual Maregraphic Station “Kalamai” [20], also in Greece, for the same period, measurements were not available for the “Kalamai” Station. The same unexpected rising of water level is observed with the passage of the medicane, something that cannot be attributed to the astronomic tides, given the acyclic behavior of this level variation. The effects caused by

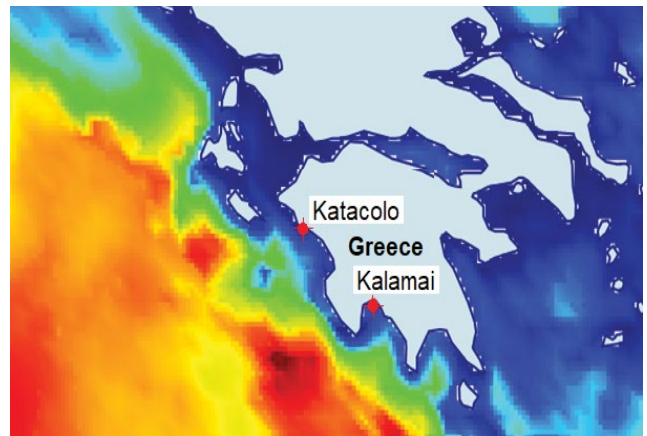


Fig. 7. Representation of the Virtual Maregraphic Stations “Kalamai” in Kalamata and “Katacolo” in Katakolon, Greece. Medicane Zorba.

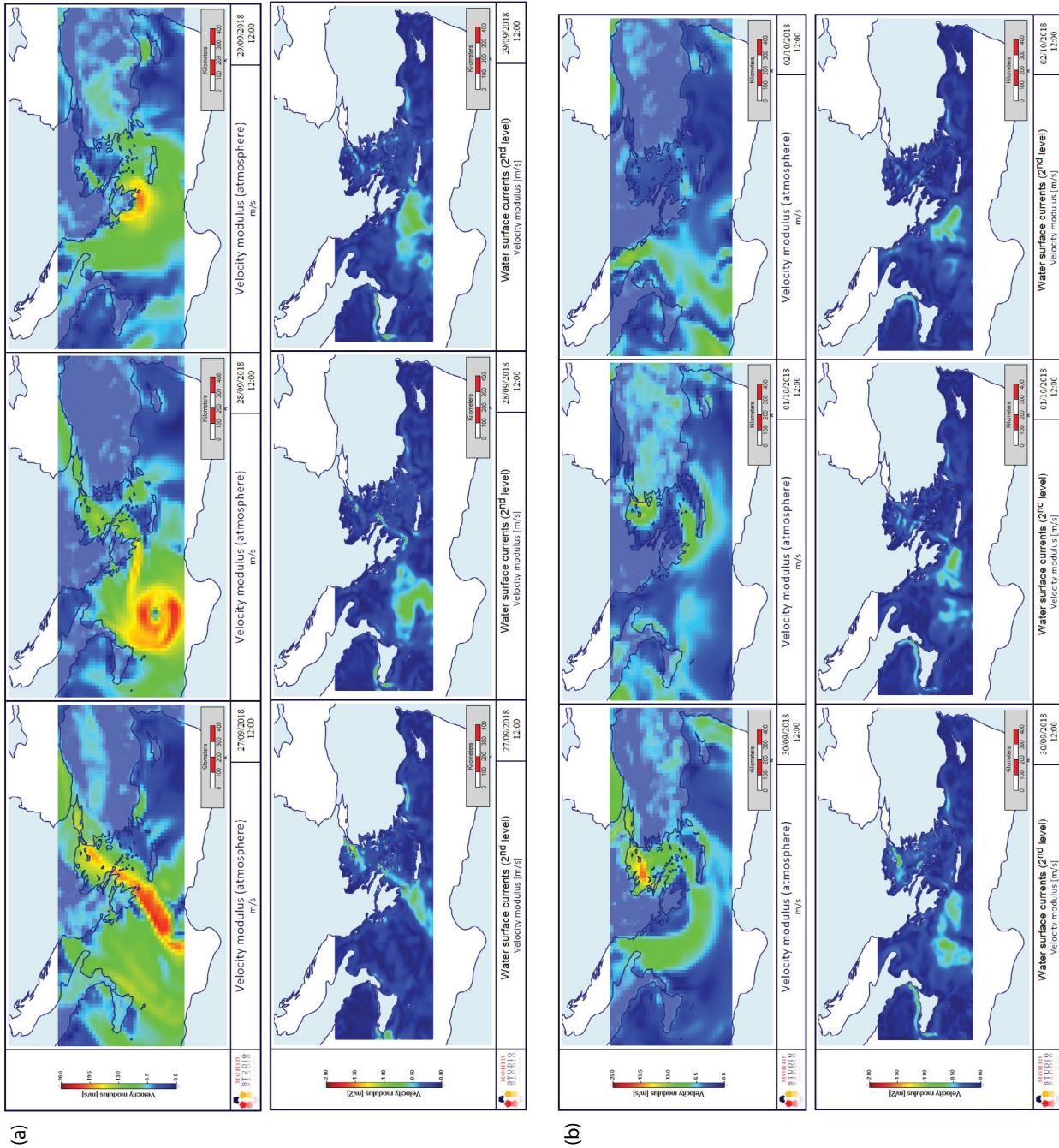


Fig. 8. Velocity moduli obtained from GFS [7] and results calculated for water surface currents with MOHID [4,5] for the Mediterranean model, for the time period (a) September 27th to 29th, 2018 and (b) September 30th to October 2nd 2018.

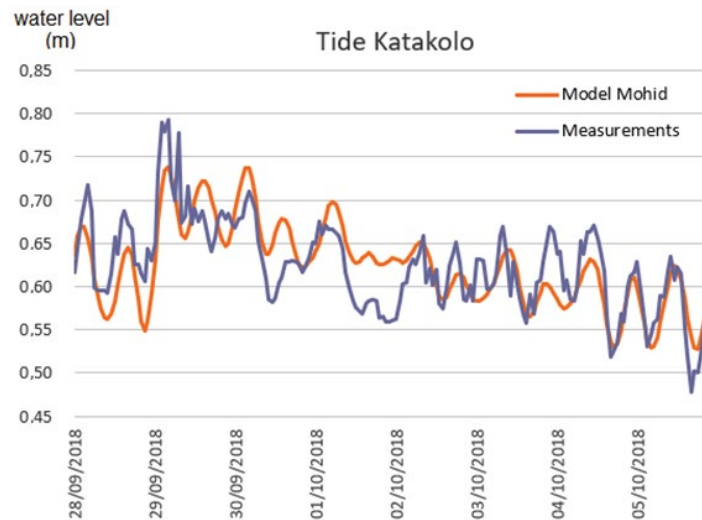


Fig. 9. Water Level measurements and model results for the Katakolo Station in Greece. Medicane Zorba.

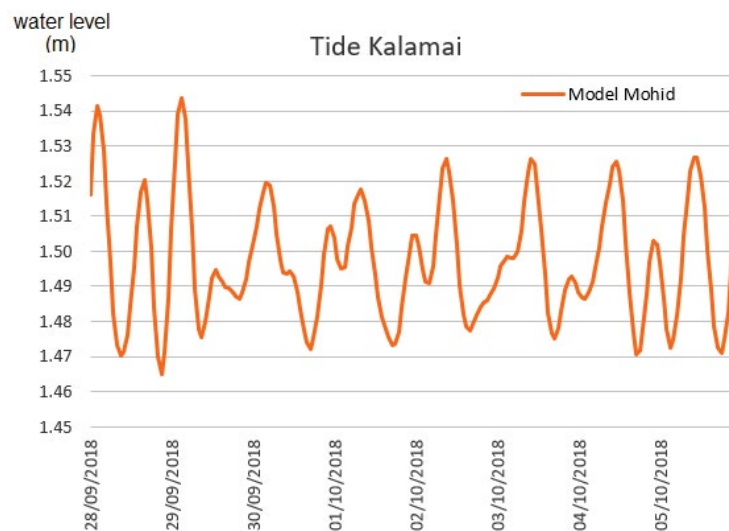


Fig. 10. Water Level Results Calculated for a Virtual Station (Kalamai) located at Kalamata, Greece.

the medicane Zorba are even more intense at Kalamai Station than at Katakolo Station, but no experimental measurements are available.

Using a notebook with an Intel® CORE® i5 5200U CPU 2.22 GHz processor with 8GB RAM, the Caribbean model required 166 h to compute the solution for the time period of 20 d, that corresponds to a performance of 0.346 model/reality coefficient, while the Mediterranean model needed 77 h to compute 8 d, with a performance of 0.388 model/reality.

4. Conclusions

The downscaling models developed for the Caribbean and Mediterranean Seas allowed the simulation of the interaction between the water and the atmosphere, resulting in the computation of the variation of the sea surface height, currents, salinity, and temperature fields. Measurements

for the water level variation at two Maregraphic Stations, one positioned along the Irma Hurricane trajectory and the other along the medicane trajectory, were compared to model results with good agreement. The results obtained are compatible with the available data from open databases and encourage the use of MOHID's platform in natural disaster modeling. The results open the possibility of using formulation and solution of inverse problems [22] for future applications that include environmental parameters estimation and drift simulation of floating objects with deterministic [23], stochastic, and hybrid methods [24,25].

Acknowledgments

The authors acknowledge the financial support provided by FAPERJ, Fundação Carlos Chagas Filho de Amparo à Pesquisa do Estado do Rio de Janeiro; CNPq, Conselho Nacional de Desenvolvimento Científico Tecnológico; and

CAPES, Coordenação de Aperfeiçoamento de Pessoal de Nível Superior (Financial Code 001) from Brazil, and the European Erasmus+ Program KA107.

Symbols

u_i	—	Velocity components in the Cartesian directions x_i
η	—	Elevation of free surface
f	—	Coriolis parameter
ν_h	—	Turbulent viscosity
p_s	—	Atmospheric pressure
ρ	—	Reference density
ρ'	—	Specific mass anomaly
ρ_η	—	Density at the free surface
η	—	Free surface elevation
h	—	Bottom depth
K	—	Diffusivities of θ
F	—	Possible sinks or sources

References

- [1] IPCC, Climate Change 2013: The Physical Science Basis, Contribution of Working Group I to the Fifth Assessment Report of the Intergovernmental Panel on Climate Change, T.F. Stocker, D. Qin, G.-K. Plattner, M. Tignor, S.K. Allen, J. Boschung, A. Nauels, Y. Xia, V. Bex, P.M. Midgley, Eds., Cambridge University Press, Cambridge, United Kingdom and New York, NY, USA, 2013, p. 1535.
- [2] J.J. González-Alemán, S. Pascale, J. Gutierrez-Fernandez, H. Murakami, M.A. Gaertner, G.A. Vecchi, Potential increase in hazard from Mediterranean hurricane activity with global warming, *Geophys. Res. Lett.*, 46 (2019) 1754–1764.
- [3] R.A. Pielkejr, C. Landsea, M. Mayfield, J. Layer, R. Pasch, Hurricanes and global warming, *Bull. Am. Meteorol. Soc.*, 86 (2005) 1571–1575.
- [4] K. Emanuel, R. Sundararajan, J. Williams, Hurricanes and global warming: results from downscaling IPCC AR4 simulations, *Bull. Am. Meteorol. Soc.*, 89 (2008) 347–367.
- [5] Y.-K. Lim, S.D. Schubert, R. Kovach, A.M. Molod, S. Pawson, The roles of climate change and climate variability in the 2017 Atlantic Hurricane season, *Sci. Rep.*, 8 (2018) 16172.
- [6] R. Romero, K. Emanuel, Medicane risk in a changing climate, *J. Geophys. Res. Atmos.*, 118 (2013) 5992–6001.
- [7] M.A. Gaertner, J.J. González-Alemán, R. Romera, M. Domínguez, V. Gil, E. Sánchez, C. Gallardo, M.M. Miglietta, K.J.E. Walsh, D.V. Sein, S. Somot, A. Dell'Aquila, C. Teichmann, B. Ahrens, E. Buonomo, A. Colette, S. Bastin, E. van Meijgaard, G. Nikulin, Simulation of medicanes over the Mediterranean Sea in a regional climate model ensemble: impact of ocean-atmosphere coupling and increased resolution, *Clim. Dyn.*, 51 (2018) 1041–1057.
- [8] ACTION MODULERS, Mohid Studio. Available at: <http://actionmodulers.pt/products/mstudio/products-mohidstudio2015.shtml> (ref. March 2, 2019).
- [9] MOHID Water Modelling System. Available at: www.mohid.com (ref. March 02, 2019).
- [10] G.A. Franz, P. Leitão, A. Santos, M. Juliano, R. Neves, From regional to local scale modelling on the south-eastern Brazilian shelf: case study of Paranaguá estuarine system, *Braz. J. Oceanogr.*, 64 (2016) 277–294.
- [11] P.M. Paiva, J. Lugon Jr., A.N. Barreto, J.F. Silva, A.J. Silva Neto, Comparing 3D and 2D computational modeling of an oil well blowout using MOHID platform – a case study in the Campos Basin, *Sci. Total Environ.*, 595 (2017) 633–641.
- [12] J. Lugon Jr., F.A. Kalas, P.P.G.W. Rodrigues, J.L. Jouveaux, H. Gallo Neto, M.M. Juliano, A.J. Silva Neto, Lagrangian trajectory simulation of floating objects in the state of São Paulo coastal region, *Defect Diffus. Forum*, 396 (2019) 42–49.
- [13] GEBCO, Gridded Bathymetry Data, General Bathymetric Chart of Oceans. Available at: https://www.gebco.net/data/_and/_products/gridded/_bathymetry/_data (ref. November 20, 2017).
- [14] GFS, GFS Analysis, Global Forecast System. Available at: <https://www.ncdc.noaa.gov/data-access/model-data/model-datasets/global-forecast-system-gfs> (ref. November 20, 2017).
- [15] L. Carrère, F. Lyard, M. Cancet, A. Guillot, L. Roblout, FES2012: A New Global Tidal Model Taking Advantage of Nearly 20 Years of Altimetry, In: *Proceedings of the Meeting 20 Years of Altimetry*, Venice, 2012.
- [16] COPERNICUS, Marine Environment Monitoring Service. Available at: http://marine.copernicus.eu/services-portfolio/access-to-products/?option=com_csw&task=results (ref. November 20, 2017).
- [17] G. Mellor, T. Yamada, Development of a turbulence closure model for geophysical fluid problems, *Rev. Geophys. Space Phys.*, 20 (1982) 851–875.
- [18] Permanent Service for Mean Sea Level (Isabella de Sagua Station). Available at: <https://www.psmsl.org/data/obtaining/stations/411.php> (ref. March 2, 2019).
- [19] Sea Level Station Monitoring Facility (Key West Station, USA). Available at: <http://www.ioc-sealevelmonitoring.org/station.php?code=kwfl> (ref. March 2, 2019).
- [20] Permanent Service for Mean Sea Level (Kalamai Station, Greece). Available at: <https://www.psmsl.org/data/obtaining/stations/411.php> (ref. March 2, 2019).
- [21] Sea Level Station Monitoring Facility (Katacolo Station, Greece). Available at: <http://www.ioc-sealevelmonitoring.org/station.php?code=kata> (ref. March 2, 2019).
- [22] F.D. Moura Neto, A.J. Silva Neto, *An Introduction to Inverse Problems with Applications*, Springer-Verlag Berlin, Heidelberg, ISBN 978-3-642-32556-4, 2013, p. 246.
- [23] J. Lugon Jr., A.J. Silva Neto, P.P.G.W. Rodrigues, Assessment of dispersion mechanisms in rivers by means of an inverse problem approach, *Inverse Prob. Sci. Eng.*, 16 (2008) 967–979.
- [24] C. Oliveira, J. Lugon Jr., D.C. Knupp, A.J. Silva Neto, A. Prieto-Moreno, O. Llanes-Santiago, Estimation of kinetic parameters in a chromatographic separation model via Bayesian inference, *Rev. Int. Métodos Numér. Cál. Diseño Ing.*, 34 (2018) 1–13.
- [25] J. Lugon Jr, A.J. Silva Neto, Solution of porous media inverse drying problems using a combination of stochastic and deterministic methods, *J. Braz. Soc. Mech. Sci. Eng.*, 33 (2011) 400–407.